Cover Page

Universiteit Leiden

Leiden University Repository

The handle http://hdl.handle.net/1887/42675 holds various files of this Leiden University dissertation.

**Author**: Thijssen, P.E.
**Title**: Genetics and epigenetics of repeat derepression in human disease
**Issue Date**: 2016-09-01

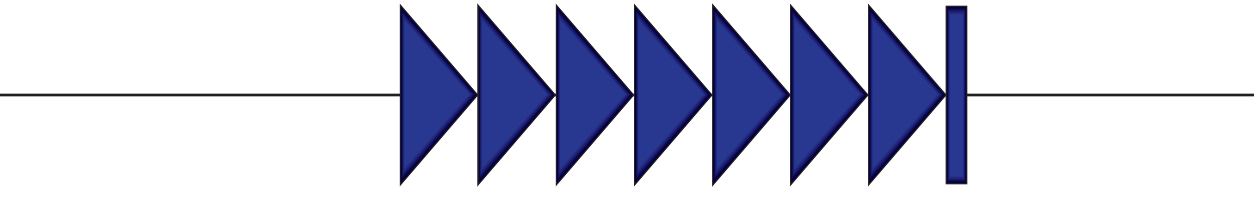

# 7

# Mutations in *CDCA7* and *HELLS* cause immunodeficiency, centromeric instability and facial anomalies syndrome.

Peter E. Thijssen, Yuya Ito, Giacomo Grillo, Jun Wang, Guillaume Velasco, Hirohisa Nitta, Motoko Unoki, Minako Yoshihara, Mikita Suyama, Yu Sun, Richard J.L.F. Lemmers, Jessica C. de Greef, Andrew Gennery, Paolo Picco, Barbara Kloeckener-Gruissem, Tayfun Güngör, Ismail Reisli, Capucine Picard, Kamila Kebaili, Bertrand Roquelaure, Tsuyako Iwai, Ikuko Kondo, Takeo Kubota, Monique M. van Ostaijen-Ten Dam, Maarten J.D. van Tol, Corry Weemaes, Claire Francastel, Silvère M. van der Maarel and Hiroyuki Sasaki

**Thijssen et al. (2015), Nature Communications, 6:7870**

## Abstract

The life threatening immunodeficiency, centromeric instability, and facial anomalies syndrome is a genetically heterogeneous autosomal recessive disorder. Twenty percent of all patients cannot be explained by mutations in the ICF genes DNA methyltransferase 3B or zinc finger and BTB domain containing 24. Here we report mutations in the cell division cycle associated 7 and the helicase, lymphoid-specific genes in ten unexplained ICF cases. Our data highlights the genetic heterogeneity of ICF syndrome and provides evidence that all genes act in common or converging pathways leading to the ICF phenotype.

## Introduction

ICF syndrome is characterized by recurrent and often fatal respiratory and gastrointestinal infections as a consequence of hypo- or a-gammaglobulinemia in the presence of B-cells[1, 2]. Nearly all patients also present with distinct facial anomalies, including hypertelorism, flat nasal bridge and epicanthus[1, 2]. Centromeric instability is the cytogenetic hallmark of ICF syndrome. It involves the juxtacentromeric heterochromatin repeats on chromosomes 1, 9, and 16 and is comparable to what is observed after treatment of cells with demethylating agents[3, 4]. Therefore, CpG hypomethylation of juxtacentromeric satellites type II and III is diagnostic for ICF syndrome, with additional hypomethylation of centromeric α-satellite repeats in *DNMT3B* mutation-negative patients[5, 6].

Mutations in the DNA methyltransferase 3B (*DNMT3B*) gene (OMIM 602900; ICF1) account for ~50% of ICF cases while ~30% of cases have mutations in the zinc finger and BTB domain containing 24 (*ZBTB24*) gene (OMIM 614064; ICF2)[2, 5]. *DNMT3B* is a de novo DNA methyltransferase, primarily acting during early development with a preference for CpG dense regions[7]. ICF1 mutations in the catalytic domain of *DNMT3B* result in largely reduced methyltransferase activity[8, 9]. The function of *ZBTB24* is unknown, but it belongs to a family of ZBTB proteins of which many have regulatory roles in hematopoietic differentiation[10, 11]. Despite the successful identification of ICF genes, the pathophysiological mechanism underlying the syndrome remains largely unresolved.

Previous studies indicated further genetic heterogeneity in ICF syndrome[2]. To identify the genetic cause in genetically unexplained cases (ICFX), we combined homozygosity mapping with whole exome sequencing. By using an autosomal recessive inheritance model and prioritizing homozygous variants in consanguineous families, we now identify four different homozygous and potentially damaging variants in the cell division cycle associated 7 (*CDCA7*) gene in five ICFX patients (now referred to as ICF3). In an additional five ICFX patients we identify compound heterozygous and homozygous variants in the helicase, lymphoid-specific (*HELLS*) gene (ICF4). We show that knock down of both new ICF genes leads to hypomethylation of juxtacentromeric heterochromatin repeats in a murine cell model. Our results emphasize the genetic heterogeneity of ICF syndrome, nonetheless provide evidence that all four ICF genes are involved in at least one common pathway.

## Results

### Missense mutations in CDCA7 cause ICF syndrome type 3

We selected 13 ICFX patients from 11 families, negative for mutations in *DNMT3B* or *ZBTB24*, of whom the clinicopathological characteristics are listed in **Table S1**. Hypomethylation of pericentromeric satellite type II (Sat II), common to all ICF patients, and centromeric α-satellite DNA repeats, shown to be affected only in ICF2 and ICFX, was shown before for a subset of patients[2, 5, 6, 12]. For an additional set of ICFX patients we confirmed Sat II and α-satellite hypomethylation using Southern blot analysis (**Fig. S1**). In five ICFX patients from four families we identified and confirmed homozygous missense mutations in *CDCA7*, all near the first two zinc finger motifs in the conserved carboxyterminal 4-CXXC-type zinc finger domain (**Fig. 1A-E**). Segregation with disease was confirmed in family D and all mutations were predicted to be pathogenic and have an allele frequency supporting pathogenicity (**Fig. 1E, Table S1**). *CDCA7* is involved in neoplastic transformation, MYC-dependent apoptosis, and hematopoietic stem cell emergence, however its molecular function is unknown[13, 14]. All four zinc finger motifs are completely conserved in the highly homologous 4-CXXC zinc finger domain of the transcriptional repressor CDCA7-Like (*CDCA7L*) (**Fig. S2**). The repressive activity of

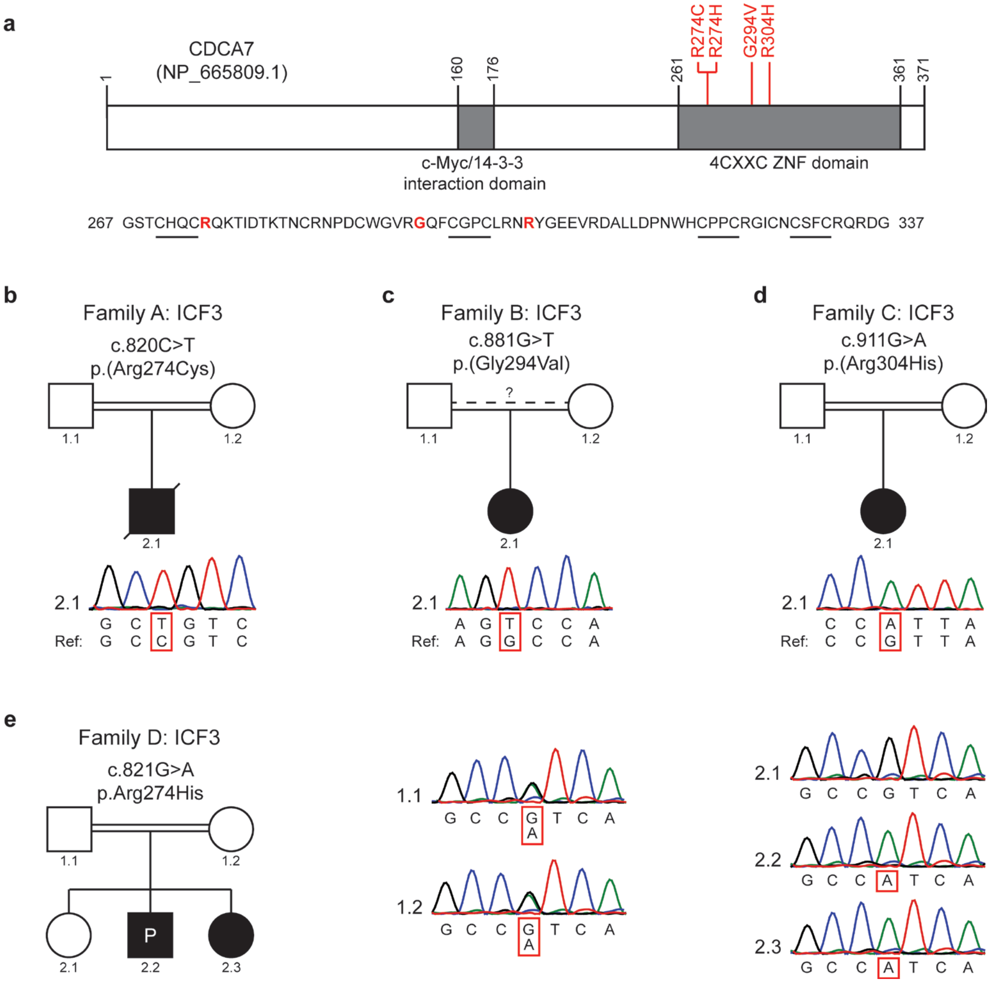
a
CDCA7
(NP_665809.1)
1
160
176
261
R274C
R274H
G294V
R304H
361
371
c-Myc/14-3-3
interaction domain
4CXXC ZNF domain
267 GSTCHQCRQKTIDTKTNCRNPDCWGVRGQFCGPCLRNRYGEEVRDALLDPNWHCPPCRGICNCSFCRQRDG 337
b
Family A: ICF3
c.820C>T
p.(Arg274Cys)
1.1
1.2
2.1
2.1
G C T G T C
Ref: G C C G T C
c
Family B: ICF3
c.881G>T
p.(Gly294Val)
?
1.1
1.2
2.1
2.1
A G T C C A
Ref: A G G C C A
d
Family C: ICF3
c.911G>A
p.(Arg304His)
1.1
1.2
2.1
2.1
C C A T T A
Ref: C C G T T A
e
Family D: ICF3
c.821G>A
p.Arg274His
1.1
1.2
P
2.1
2.2
2.3
1.1
G C C G/A T C A
1.2
G C C G/A T C A
2.1
G C C G T C A
2.2
G C C A T C A
2.3
G C C A T C A

**Figure 1: Homozygous missense mutations in *CDCA7* in five ICF3 patients.**
**A)** Schematic representation of CDCA7, with the identified homozygous missense mutations in red. Sequence outtake: 4-CXXC type zinc finger domain, CXXC motifs are underlined, mutated residues in red. **B-D)** Sanger sequencing confirmation of missense mutations in *CDCA7* in families A-C. All variants were homozygous, the reference sequence is displayed for comparison. **E)** Sanger sequencing confirmation of the homozygous missense *CDCA7* mutation in patients 2.2 (proband) and 2.3 of family D. Both parents are heterozygous for the variant, sibling 2.1 is unaffected and homozygous for the wild type allele.

CDCA7L is dependent on its 4-CXXC domain and by homology CDCA7 mutations in ICF3 may disrupt a similar function[15].

### Mutations in HELLS cause ICF syndrome type 4

In an additional five ICFX patients from four families we identified mutations in *HELLS* that were predicted to be pathogenic and with allele frequencies supporting pathogenicity (**Fig. 2A, Table S1**, ICF4). In affected members of family E we identified a missense mutation in the conserved helicase domain (c.2096A>G; p.Gln699Arg) and an intronic mutation leading to destruction of the splice donor site in intron 5 (c.370+2T>A) (**Fig. 2B**). Different allelic origin is supported by analysis of maternal DNA, which carried only the splice site mutation (**Fig. 2C**). To analyse the effect of the lost splice donor site on mRNA processing, fibroblasts of both patients were treated with cycloheximide to inhibit nonsense mediated decay. Upon treatment, RT-PCR analysis showed increased levels of a splice variant with complete skipping of exon 5, leading to a frameshift followed by a premature stop codon in exon 6 (**Fig. 2C**).

The patient in family F carries a homozygous out-of-frame deletion (c.2283_2286delGTCT; p.[Ser762Argfs*4]), resulting in a frameshift and introduction of a premature stop codon in exon 20. The unaffected siblings 2.1 and 2.3 were found to be heterozygous for the deletion or homozygous for the wild type allele, respectively (**Fig. 2D**). In family G we found a deleterious homozygous in-frame deletion in the C-terminal domain of HELLS, leading to the deletion of Leucine 801 (c.2400_2402delGTT; p.[Leu801del]) (**Fig. 2E**). The proband of family H carries a nonsense mutation (c.610A>T; p.[Lys204*]) and a duplication causing the insertion of a stop codon (c.374_381dup; p.[Lys128*]), suggesting that absence of HELLS is compatible with human life, whereas *Hells*$^{-/-}$ mice die perinatally16. Different allelic origin of the mutations was confirmed in parental DNA (**Fig. 2F**).

### ICF genes converge at centromeric DNA methylation regulation

In mouse, HELLS is required for T-cell proliferation and mediates de novo DNA methylation, through its interaction with DNMT3B, dependent on its ATPase domain[16-19]. Genome wide loss of CpG methylation, including centromeric repeats, has been observed in *Hells*$^{-/-}$ mice, reminiscent of what has been described in *Dnmt3b* knockout mice and in mouse models for ICF1[20, 21]. We show that transient depletion of HELLS, CDCA7 and ZBTB24, but not DNMT3B, resulted in decreased CpG methylation at centromeric repeats in wild type (wt) mouse embryonic fibroblasts (MEFs, **Fig. 2G, Fig. S2A-B**). This confirms that DNMT3B acts during establishment of centromeric CpG methylation[22]. Moreover, it supports a role for ZBTB24 and CDCA7 in maintenance of CpG methylation at centromeric repeats, and, combined with previously published work, suggests that HELLS may be involved in both processes[19].

By identifying two new ICF syndrome genes this study highlights its genetic heterogeneity, and the identification of at least one additional disease gene is expected with still a few cases remaining genetically unresolved. The complex, but highly overlapping pathophysiology suggests that all ICF genes act in common or converging pathways involved in immunity, chromatin regulation and development. Convergence is supported by hypomethylation of pericentromeric repeats, common to all ICF subgroups, however the result of different defective pathways in the establishment and/or maintenance of CpG methylation.

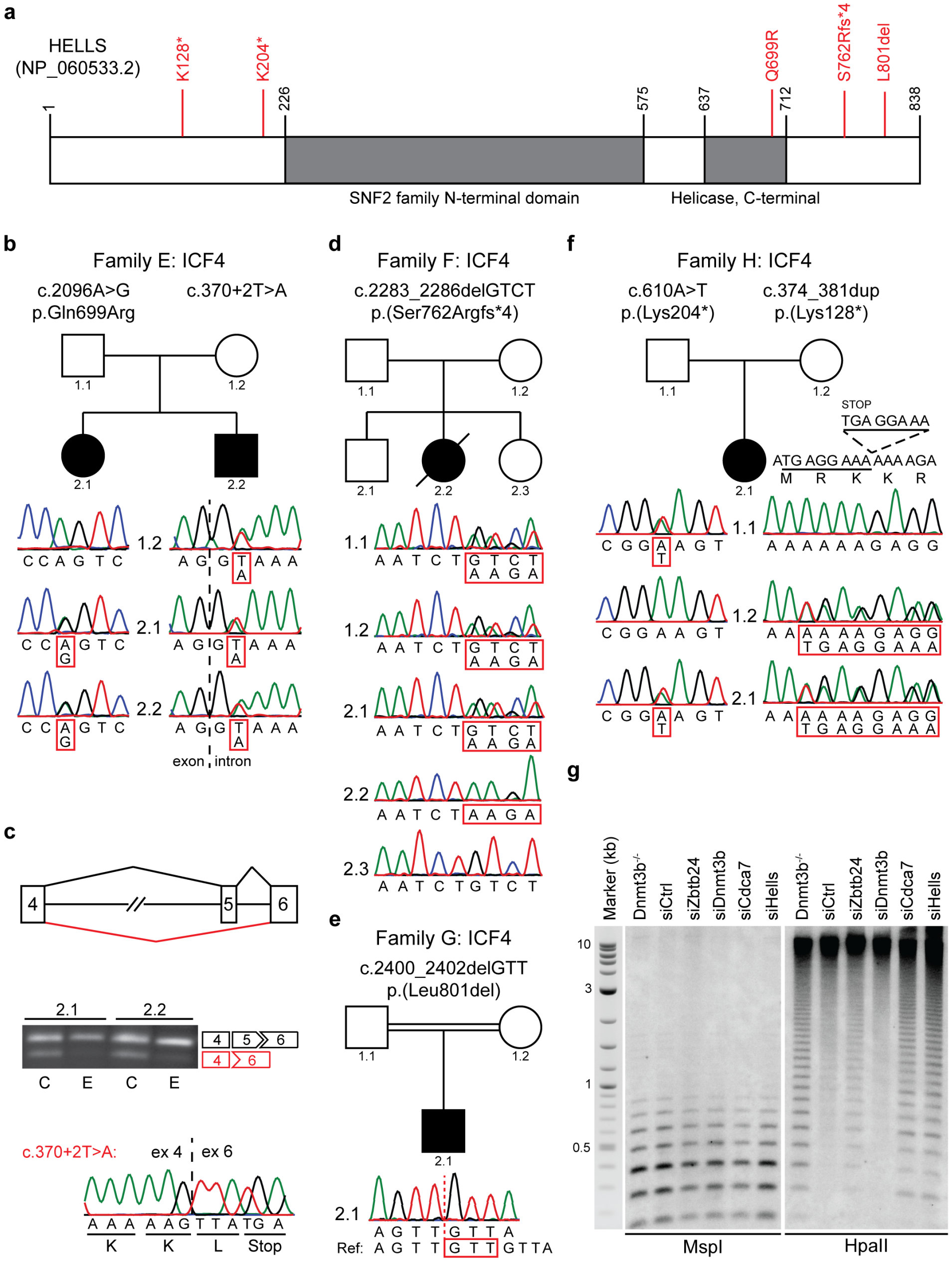
a
HELLS
(NP_060533.2)
K128*
K204*
Q699R
S762Rfs*4
L801del
1
226
575
637
712
838
SNF2 family N-terminal domain
Helicase, C-terminal
b
Family E: ICF4
c.2096A>G
p.Gln699Arg
c.370+2T>A
1.1
1.2
2.1
2.2
C C A G T C
A G G T A A A
exon
intron
c
4
5
6
2.1
2.2
C E C E
c.370+2T>A:
ex 4
ex 6
A A A A A G T T A TG A
K K L Stop
d
Family F: ICF4
c.2283_2286delGTCT
p.(Ser762Argfs*4)
A A T C T G T C T
A A G A
e
Family G: ICF4
c.2400_2402delGTT
p.(Leu801del)
A G T T G T T A
Ref: A G T T G T T G T T A
f
Family H: ICF4
c.610A>T
p.(Lys204*)
c.374_381dup
p.(Lys128*)
STOP
TGA GGA AA
ATG AGG AAA AAA AGA
M R K K R
C G G A A G T
A A A A A A G A G G
T G A G G A A A
g
Marker (kb)
Dnmt3b-/-
siCtrl
siZbtb24
siDnmt3b
siCdca7
siHells
10
3
1
0.5
MspI
HpaII

# Methods

## Patients

All samples were obtained in an anonymized fashion and all families gave consent for genetic analyses. The study was approved by the Medical Ethical Committee of the Leiden University Medical Center, the local ethics committee of Necker-Enfants Malades Hospital, Paris, France and the Kyushu University Institutional Review Board for Human Genome/Gene Research. The patient from family A (referred to as patient 2 in Kloeckener-Gruissem et. al., 2005), patients from families B and C (referred to as pC and pS, respectively, in Velasco et. al., 2014), patient 2.2 from family D, and the patients in family E (referred to as P4 and P8/P9, respectively, in De Greef et. al., 2011), as well as the three remaining ICFX cases (referred to as pN and P1 in Velasco et. al., 2014 and P4 in Kubota et. al., 2004) all show typical clinical features of ICF syndrome including hypo- or agammaglobulinemia in the presence of B cells, combined with the classical cytogenetic abnormalities involving chromosomes 1, 9 and 16, and hypomethylation of α-satellite DNA in addition to SatII hypomethylation. The critical features of all patients are summarized in supplementary table 1, further details can be found in previous descriptions of these patients[2, 5, 6, 12, 23, 24].

## Gene identification by homozygosity mapping and sequencing

Homozygosity mapping was performed using the Sentrix HumanHap-300 Genotyping BeadChips (Illumina). To this end, 750ng genomic DNA was processed with the Infinium II Whole-Genome Genotyping Assay (Illumina). After DNA amplification, fragmentation, precipitation and resuspension, DNA was applied to the BeadChip and incubated overnight, followed by enzymatic base extension, fluorescent staining of the beads, and detection of fluorescent intensities by the BeadArray Reader (Illumina). To identify regions of homozygosity, B allele frequencies were assessed for all SNPs using BeadStudio version 3.2 (Illumina). For a subset of patients, whole exome sequencing was performed in the Neuromics project by deCODE Genetics (Reykjavik – Iceland) and analyzed using deCODE Clinical Sequence Miner. Recessive analysis for multiple cases and controls and gene variant effect count (with VEP consequences moderate to high) were used

**Figure 2: Mutations in HELLS in five ICF4 patients.**
**A)** Schematic representation of HELLS, with the identified mutations in red. **B)** Sanger sequencing confirmation of *HELLS* mutations in family E. Only c.370+2T>A was identified in maternal DNA, indicating different allelic origin of both mutations, or de novo occurrence of the second mutation. **C)** RT-PCR analysis of HELLS mRNA upon treatment of patient derived fibroblasts with cycloheximide (C) revealed that c.370+2T>A leads to complete skipping of exon 5 and disruption of the open reading frame. Ethanol treated samples (E) served as controls, alternative splicing was confirmed by Sanger sequencing in two independent experiments for both samples. **D)** Sanger sequencing confirmation of a homozygous out-of-frame deletion in *HELLS* in family F. Both parents, as well as unaffected sibling 2.1 are heterozygous for the deletion allele, unaffected sibling 2.3 is homozygous for the wildtype allele. **E)** Sanger sequencing confirmation of a homozygous in-frame deletion in *HELLS* in family G. Both parents are heterozygous for the deletion allele. **F)** Sanger sequencing confirmation of nonsense mutations in *HELLS* in family H. Different allelic origin was confirmed in parental DNA. **G)** Southern blot analysis of minor satellite DNA methylation in wt, *Dnmt3b*$^{-/-}$ and siRNA-treated wt MEFs after digesting DNA with MspI or its methylation sensitive isoschizomer HpaII revealed CpG hypomethylation upon knockdown of Zbtb24, Cdca7 and Hells. Molecular weights of the 2-Log DNA size marker are in kilo-basepairs.

to identify possible recessive mutations. For an additional set of patients, DNA libraries for whole exome sequencing were constructed using the SureSelect Human All Exon V5 kit (Agilent Technologies) according to the manufacturer's instructions. Sequencing was performed on the Illumina HiSeq2500 platform to generate 100bp paired-end reads. Reads were mapped to the reference human genome (UCSC hg19) with the Burrows-Wheeler Alignment tool (BWA v0.7.4)25. Duplicate reads were removed by Picard (v1.87). We called SNVs and indels using the Genome Analysis Toolkit (GATK v2.5-2)26. Annotations of variants were made using ANNOVAR27. For confirmation, relevant exons and flanking sequences of *CDCA7* and *HELLS* were amplified using standard PCR, products were purified and analysed by Sanger sequencing. Sequence tracks were analysed and visualized using ContigExpress (Vector NTI, Invitrogen-Life Technologies). PCR primers are listed in **table S2**.

**Cycloheximide treatment and RT-PCR analysis**

Early passage (p<6) patient derived primary fibroblast were maintained in DMEM F12 (31331) supplemented with 20% heat inactivated Fetal Calf Serum, 1% pen-strep, 1% sodium pyruvate and 1% HEPES (all Invitrogen-Life Technologies). Cells were treated with 250 µg ml^-1 cycloheximide (dissolved in ethanol, 01810, Sigma-Aldrich) for 4 hours using equal volumes of ethanol as control. After treatment, cells were harvested in Qiazol lysis reagent and RNA was isolated using the miRNeasy mini kit (both Qiagen) all according to manufacturer's instructions. 2 µg of total RNA was used for random primed cDNA synthesis using the RevertAid first-strand cDNA synthesis kit (Thermo scientific). Transcripts were amplified by standard PCR with primers listed in supplementary table 2, separated by standard gel electrophoresis and sequenced by Sanger sequencing.

**Knockdown of gene expression in MEFs**

The use of animal work has been reviewed by the Animal Experimentation Ethical Committee Buffon (CEEA-40), Paris, France, and approved under the number CEB-06-2012. Female C57BL/6N pregnant mice, age 3 to 6 months, were sacrificed at 12.5 dpc, and individual mouse embryonic fibroblasts (MEF) clones isolated from each embryo of the litter. Primary MEFs were cultivated for no more than 2-3 passages in complete media (DMEM glutamax supplemented with 10% FBS, 100 U mL^-1 penicillin, 100 µg mL^-1 streptomycin, all from Life Technologies). Two rounds of transfection with synthetic siRNAs at a final concentration of 20 nM were performed using Interferin transfection reagent (Polyplus-transfection) following the manufacturer's instructions: a first round on MEFs in suspension and the second when cells were allowed to adhere to the plate. Cells were collected after 48 hours for genomic DNA extraction. Sequences of siRNAs used in the study are listed in **Table S2**.

**Satellite DNA methylation analysis by Southern blotting**

Satellite II and α-satellite methylation in whole blood DNA was analysed by Southern blot analysis of 2µg genomic DNA digested with methylation-sensitive restriction enzymes HhaI for analysis of Sat-α or BstBI for analysis of SatII repeats. Both enzymes were purchased from Fermentas. After overnight digestion, DNA was separated by electrophoresis using 0.8% agarose gels. DNA was transferred overnight to Hybond-N+

membranes (GE Healthcare) and hybridized with a radioactive probes recognizing the α-satellite and satellite II repeats, respectively. Signals were detected by phosphoimaging or by exposure to X ray films. For analysis of murine satellite repeats, genomic DNA was extracted and purified from MEFs using the NucleoSpin®Tissue kit (Macherey-Nagel) according to manufacturer's instructions. The DNA pellet was eluted in TE containing 20 µg mL^-1 RNAse A. Genomic DNA from MEFs (500 ng) was digested with 20 units of MspI or HpaII (New England Biolabs) for 16h to analyze the DNA methylation patterns of centromeric minor satellite repeats. The digested DNA fragments were separated by electrophoresis using 1% agarose gels and transferred overnight to Hybond-N+ membranes (GE Healthcare) in 20XSSC. After UV-crosslink, the membranes were pre-hybridized in 6X SSC, 5X Denhardt and 0.1% SDS and then hybridized with 32P-labeled minor satellite oligonucleotide probe:
(5'-ACATTCGTTGGAAACGGGATTTGTAGAACAGTGTATATCAATGAGTTACAATGAGAAACAT). Pre-hybridization and hybridization were carried out at 42°C for 1h. The membranes were washed 3 times in 6X SSC and 0.1%SDS at 37°C and signals detected by phosphorimaging using FLA 7000 phosphorimager (Fuji). Uncropped scans of the Southern blots are presented in **Figs. S4-S5**.

### Quantification of knockdown efficiency by qRT-PCR

Total RNA from MEFs was isolated using TRIzol® Reagent (Life Technologies) according to manufacturer's instructions. Contaminant genomic DNA was eliminated with TURBO DNA-free kit (Ambion). Reverse transcription was carried out using 1 µg DNA-free RNA and 50 µM random hexamers, 20U of RNase Out and 100U of RevertAid reverse transcriptase (Life Technologies). Complementary DNA reactions were used as templates for PCR reactions. Real-time PCR was performed using the light cycler-DNA MasterPLUS SYBR Green I mix (Thermo Scientific) supplemented with 0.5 µM of specific primer pairs (listed in supplementary table 2). Real-time quantitative PCRs were run on a light cycler rapid thermal system (LightCycler®480 2.0 Real time PCR system, Roche) with 20 sec of denaturation at 95°C, 20 sec of annealing at 60°C and 20 sec of extension at 72°C for all primers, and analyzed by the comparative CT (ΔCT) method.

## References

1. Hagleitner,M.M. et al. Clinical spectrum of immunodeficiency, centromeric instability and facial dysmorphism (ICF syndrome). J. Med. Genet. 45, 93-99 (2008).
2. Weemaes,C.M. et al. Heterogeneous clinical presentation in ICF syndrome: correlation with underlying gene defects. Eur. J. Hum. Genet. 21, 1219-1225 (2013).
3. Jeanpierre,M. et al. An embryonic-like methylation pattern of classical satellite DNA is observed in ICF syndrome. Hum. Mol. Genet. 2, 731-735 (1993).
4. Tiepolo,L. et al. Multibranched chromosomes 1, 9, and 16 in a patient with combined IgA and IgE deficiency. Hum. Genet. 51, 127-137 (1979).
5. de Greef,J.C. et al. Mutations in ZBTB24 are associated with immunodeficiency, centromeric instability, and facial anomalies syndrome type 2. Am. J. Hum. Genet. 88, 796-804 (2011).
6. Jiang,Y.L. et al. DNMT3B mutations and DNA methylation defect define two types of ICF syndrome. Hum. Mutat. 25, 56-63 (2005).
7. Auclair,G., Guibert,S., Bender,A., & Weber,M. Ontogeny of CpG island methylation and specificity of DNMT3 methyltransferases during embryonic development in the mouse. Genome Biol. 15, 545 (2014).
8. Gowher,H. & Jeltsch,A. Molecular enzymology of the catalytic domains of the Dnmt3a and Dnmt3b DNA methyltransferases. J. Biol. Chem. 277, 20409-20414 (2002).
9. Moarefi,A.H. & Chedin,F. ICF syndrome mutations cause a broad spectrum of biochemical defects in DNMT3B-mediated de novo DNA methylation. J. Mol. Biol. 409, 758-772 (2011).
10. Nitta,H. et al. Three novel ZBTB24 mutations identified in Japanese and Cape Verdean type 2 ICF syndrome patients. J. Hum. Genet. 58, 455-460 (2013).
11. Lee,S.U. & Maeda,T. POK/ZBTB proteins: an emerging family of proteins that regulate lymphoid development and function. Immunol. Rev. 247, 107-119 (2012).
12. Velasco,G. et al. Germline genes hypomethylation and expression define a molecular signature in peripheral blood of ICF patients: implications for diagnosis and etiology. Orphanet. J. Rare. Dis. 9, 56 (2014).
13. Gill,R.M., Gabor,T.V., Couzens,A.L., & Scheid,M.P. The MYC-associated protein CDCA7 is phosphorylated by AKT to regulate MYC-dependent apoptosis and transformation. Mol. Cell Biol. 33, 498-513 (2013).
14. Guiu,J. et al. Identification of Cdca7 as a novel Notch transcriptional target involved in hematopoietic stem cell emergence. J. Exp. Med.(2014).
15. Chen,K., Ou,X.M., Wu,J.B., & Shih,J.C. Transcription factor E2F-associated phosphoprotein (EAPP), RAM2/CDCA7L/JPO2 (R1), and simian virus 40 promoter factor 1 (Sp1) cooperatively regulate glucocorticoid activation of monoamine oxidase B. Mol. Pharmacol. 79, 308-317 (2011).
16. Geiman,T.M. & Muegge,K. Lsh, an SNF2/helicase family member, is required for proliferation of mature T lymphocytes. Proc. Natl. Acad. Sci. U. S. A 97, 4772-4777 (2000).
17. Ren,J. et al. The ATP binding site of the chromatin remodeling homolog Lsh is required for nucleosome density and de novo DNA methylation at repeat sequences. Nucleic Acids Res. 43, 1444-1455 (2015).
18. Yu,W. et al. Genome-wide DNA methylation patterns in LSH mutant reveals de-repression of repeat elements and redundant epigenetic silencing pathways. Genome Res. 24, 1613-1623 (2014).
19. Zhu,H. et al. Lsh is involved in de novo methylation of DNA. EMBO J. 25, 335-345 (2006).
20. Ueda,Y. et al. Roles for Dnmt3b in mammalian development: a mouse model for the ICF syndrome. Development 133, 1183-1192 (2006).
21. Velasco,G. et al. Dnmt3b recruitment through E2F6 transcriptional repressor mediates germ-line gene silencing in murine somatic tissues. Proc. Natl. Acad. Sci. U. S. A 107, 9281-9286 (2010).
22. Okano,M., Bell,D.W., Haber,D.A., & Li,E. DNA methyltransferases Dnmt3a and Dnmt3b are essential for de novo methylation and mammalian development. Cell 99, 247-257 (1999).
23. Kloeckener-Gruissem,B., Betts,D.R., Zankl,A., Berger,W., & Gungor,T. A new and a reclassified ICF patient without mutations in DNMT3B and its interacting proteins SUMO-1 and UBC9. Am. J. Med. Genet. A 136, 31-37 (2005).
24. Kubota,T. et al. ICF syndrome in a girl with DNA hypomethylation but without detectable DNMT3B

mutation. Am. J. Med. Genet. A 129A, 290-293 (2004).

25. Li,H. & Durbin,R. Fast and accurate long-read alignment with Burrows-Wheeler transform. Bioinformatics. 26, 589-595 (2010).
26. McKenna,A. et al. The Genome Analysis Toolkit: a MapReduce framework for analyzing next-generation DNA sequencing data. Genome Res. 20, 1297-1303 (2010).
27. Wang,K., Li,M., & Hakonarson,H. ANNOVAR: functional annotation of genetic variants from high-throughput sequencing data. Nucleic Acids Res. 38, e164 (2010).

## Acknowledgements

We thank all patients and their families for their consent tp contribute to our study. We thank K. Ichiyanagi and L. Daxinger for helpful advice, staff of Kyushu University International Legal Office for help in legal and ethical affairs, and T.P. Pham, S.L. Höcker, M. Miyake and H. Furuumi for technical assistance. This work was supported by KAKENHI (22134006, 23249019, and 26253020), the National Institutes of Health/National Institute of Allergy and Infectious Diseases (R21 AI090135), European Community's Seventh Framework Programme (FP7/2007-2013) under grant agreement n° 2012-305121 "Integrated European –omics research project for diagnosis and therapy in rare neuromuscular and neurodegenerative diseases (NEUROMICS)" and French National Research Agency – Program on physiopathology of rare diseases (ANR-09-GENO-035).

## Competing financial interests

The authors declare to have no competing financial interests.

## Accession Codes

Sequence data have been deposited to the Leiden Open Variation Database (LOVD):
http://databases.lovd.nl/shared/individuals/CDCA7
http://databases.lovd.nl/shared/individuals/HELLS

## Supplementary information

**Fig. S1:** Repeat hypomethylation in ICF patients from families E, F and G
**Fig. S2:** Aligment of the 4-CXXC domains of CDCA7 and CDCA7L
**Fig. S3:** Confirmation of minor satellite hypomethylation through siRNA mediated knockdown in wildtype MEFs
**Fig. S4:** Uncropped images of agarose gels and Southern blots corresponding to Figure 2g
**Fig. S5:** Uncropped images of agarose gels and Southern blots corresponding to Supplementary Figure 3b

**Table S1:** Demographic and clinical characteristics of patients
**Table S2:** List of primers and siRNAs

All supplementary information belonging to this chapter can be accessed through http://goo.gl/ynEKdX or by using the QR-code below.